Preparation and properties of superconducting $La_{1+x}Ba_{2-x}Cu_3O_y$ $(0 \leq x \leq 0.5)$ ceramics sintered in N_2 gas atmosphere

Takahiro Wada
Central Research Laboratory, Matsushita Electric Industrial Corporation Ltd., Moriguchi, Osaka 570, Japan

Nobuo Suzuki
Engineering Research Center, Tokyo Electric Power Company, Choufu, Tokyo 182, Japan

Atsutaka Maeda, Tomoaki Yabe, and Kunimitsu Uchinokura
Department of Applied Physics, University of Tokyo, Hongo, Bunkyo-ku, Tokyo 113, Japan

Shin-ichi Uchida
Engineering Research Institute, University of Tokyo, Yayoi, Bunkyo-ku, Tokyo 113, Japan

Shoji Tanaka
International Superconductivity Technology Center, Shinbashi, Minato-ku, Tokyo 105, Japan
and Department of Physics, Tokai University, Hiratsuka, Kanagawa 259-12, Japan
(Received 13 December 1988)

A study of the preparation and properties of $La_{1+x}Ba_{2-x}Cu_3O_y$ $(0 \leq x \leq 0.5)$ system was performed on two kinds of samples. One with $0 \leq x \leq 0.2$ was sintered at 970–980 °C in N_2 gas and postannealed at 300 °C in O_2 gas atmosphere and the other with $0 \leq x \leq 0.5$ was sintered at 900 °C in N_2 gas and postannealed under the same conditions. The samples sintered at 970–980 °C were orthorhombic and their oxygen content (y) was nearly 6.95, smaller than that of those sintered at 900 °C, which was about 7.15. Thermogravimetric study revealed that samples sintered at 900 °C contained a large amount of oxygen; the oxygen content was not substantially reduced at elevated temperature, even in N_2 gas atmosphere. Resistivity and dc magnetic-susceptibility measurements revealed that the superconducting properties of the samples sintered at 970–980 °C were much better than those of the samples sintered at lower temperature. The T_c's in the $La_{1+x}Ba_{2-x}Cu_3O_y$ system with $y \approx 7.0$ decreased linearly from 93 to 80 K with excess La content, x. Differential scanning calorimetry in O_2 gas atmosphere showed that the orthorhombic-tetragonal structural phase transition temperatures were lowered monotonically from 485 °C ($x=0$) to 443 °C ($x=0.3$). We address the effect of La substitution for Ba in $LaBa_2Cu_3O_{7.0}$ samples on their superconducting properties. We discuss the relation between the oxygen content in $La_{1+x}Ba_{2-x}Cu_3O_y$ samples and their superconducting properties. Finally, we discuss the reasons why the superconducting properties of the samples which were sintered in N_2 gas are better than those of the samples sintered in O_2 gas or air.

I. INTRODUCTION

$LaBa_2Cu_3O_y$ has an orthorhombic[1,2] oxygen-deficient triperovskite structure and is isostructural to $YBa_2Cu_3O_y$, in which Ba^{2+} and Y^{3+} have an ordered arrangement (Ba-Y-Ba) along the c axis and the occupation factor of oxygen ions at $(\frac{1}{2},0,0)$ and $(0,\frac{1}{2},0)$ are close to 0 and 1, respectively.[3–7] Like $YBa_2Cu_3O_y$, this material shows bulk superconductivity above 90 K.[1] However, the highest zero-resistance temperature reported so far is about 80 K.[1,8–10] Recently, we have synthesized good-quality $LaBa_2Cu_3O_y$ by sintering above 950 °C in N_2 gas and postannealing in dry O_2.[11,12] One sample showed a superconducting transition with an onset at 93 K and zero resistance at 92 K. Among the series of 90-K superconductors $LBa_2Cu_3O_y$ (where L is Y or lanthanide), $LaBa_2Cu_3O_y$ has attracted attention because the cost of La is among the lowest of the lanthanide elements.

The La-Ba-Cu-O phase diagram includes a solid solution region with the formula $La_{1+x}Ba_{2-x}Cu_3O_y$ $[La(Ba_{1-x/2}La_{x/2})_2Cu_3O_y]$[10,13–16] because of the similarity in the ionic radii of La^{3+} (1.27 Å) and Ba^{2+} (1.52 Å).[17] Homogeneous single-phase samples can be prepared in the range from $x=0.1$ and $x=0.6$.[13,14] Single-phase $LaBa_2Cu_3O_y$ ($x=0$) has not been synthesized by any technique other than ours. X-ray-powder-diffraction patterns of the samples with $x=0.1$ could be indexed to an orthorhombic unit cell; samples with $0.2 \leq x \leq 0.6$ were tetragonal.[10,16] The superconducting transition temperatures (T_c) of $La_{1+x}Ba_{2-x}Cu_3O_y$ samples were lowered from about 85 K ($x=0$) to about 40 K ($x=0.3$) with increasing La content.[10] From a neutron-powder diffraction study, Segre *et al.*[15] determined the occupation factor of oxygen in $(\frac{1}{2},0,0)$ and $(0,\frac{1}{2},0)$ sites for several samples with different T_c and suggested that the T_c was intimately connected to the presence of ordered Cu-O chains.

However, all the samples in the $La_{1+x}Ba_{2-x}Cu_3O_y$

series studied so far were sintered in air or O_2. Their quality was not evaluated by the dc magnetic-susceptibility measurements. There are few discussions of the relation between their oxygen contents and superconducting properties. Further, reports on the orthorhombic-tetragonal structural phase transition in $La_{1+x}Ba_{2-x}Cu_3O_y$ system are hard to find in spite of the great practical and scientific importance of this topic.

In this paper, we present an extensive study on the preparation and properties of $La_{1+x}Ba_{2-x}Cu_3O_y$ ($0 \leq x \leq 0.5$) samples. We prepared high-T_c superconducting $La_{1+x}Ba_{2-x}Cu_3O_y$ solid solution samples by sintering in N_2 gas and postannealing in dry O_2. We have found from the study of preparation of high-quality $LaBa_2Cu_3O_y$ (Ref. 11) that the quality of the samples sintered in N_2 gas and postannealed in dry O_2 gas is much better than that of previously reported samples, which were sintered in air or O_2 gas.

The identification of the phases and the determination of the lattice parameters were performed by x-ray-powder diffraction. Discrimination between orthorhombic and tetragonal region of samples was performed using a polarized optical microscope and a transmission electron microscope as well as by x-ray-powder diffraction. High-resolution transmission electron microscopic (HRTEM) analysis was performed to study the structure of the tetragonal sample with $x=0.2$. The oxygen content was analyzed by the inert gas fusion nondispersive ir method. Oxygen desorption and absorption in the samples at elevated temperatures were studied by means of thermogravimetry (TG). In order to evaluate the bulk superconductivity, dc-magnetic susceptibility measurements were carried out. Resistivity measurements were also performed. The orthorhombic-tetragonal phase transition temperature was determined using differential scanning calorimetry (DSC).

We will discuss the following three points. The first is the effect of La^{3+} substitution for Ba^{2+} in $LaBa_2Cu_3O_y$ samples on their superconducting properties, as compared with the case of $YBa_{2-x}La_xCu_3O_y$.[18] The second is the relation between the oxygen content of the samples and their superconducting properties. Finally, we discuss the reason why the superconducting properties of samples sintered at 970–980 °C in N_2 gas and postannealed in dry O_2 gas are so much better than those of the previously reported samples which were sintered in air or O_2 gas. The discussion is based on the results of TG measurements in N_2 and O_2.

II. EXPERIMENTAL PROCEDURE

$La_{1+x}Ba_{2-x}Cu_3O_y$ ($0 \leq x \leq 0.5$) ceramics were prepared from La_2O_3, $BaCO_3$, and CuO powders. The synthetic procedure for $LaBa_2Cu_3O_y$ was reported in detail in a previous paper.[11] The La_2O_3 was used after being prefired at 1000 °C for 5 h in air because it is hygroscopic.[12] These powders were ball milled in ethanol and calcined at 900 °C for 5 h in air. The resulting black powder was ground and recalcined at 950 °C for 10 h in air. The calcined powder was molded and sintered at 900–980 °C for 40 h in various atmospheres. The sintered ceramics were postannealed at 300 °C for 40 h in dry O_2. The starting composition and synthesis conditions for the samples were summarized in Table I.

The phases present and their lattice parameters were determined by x-ray-powder diffraction using Cu $K\alpha$ radiation. For structural refinement, a curved graphite monochromator was placed in the scattering beam path. Lattice parameters were determined by Cohen's method.[19]

The oxygen content of the sample was analyzed by an inert gas fusion nondispersive ir method (Horiba Seisakusho model EMGA-2800). A weighed quantity of the sample (about 50 mg) and flux (nickel and tin) were placed in a carbon crucible. When the sample was heated to fusion in He gas, all the oxygen in the sample reacted with carbon and carbon monoxide gas was produced. The quantity of carbon monoxide produced was analyzed by an infrared spectrometer. High-purity (99.99%) Y_2O_3 was used as a standard sample. All the results shown in

TABLE I. The compositions and preparation conditions of samples in the $La_{1+x}Ba_{2-x}Cu_3O_y$ series.

Sample No.	Composition x	Sintering condition Temperature (°C)	Atmosphere
1	0.00	980	N_2
2	0.05	970	N_2
3	0.10	970	N_2
4	0.20	970	N_2
5[a]	0.30	970	N_2
6	0.00	900	N_2
7	0.05	900	N_2
8	0.10	900	N_2
9	0.20	900	N_2
10	0.30	900	N_2
11	0.40	900	N_2
12	0.50	900	N_2
13	0.10	970	Ar
14	0.10	970	air

[a]This sample was annealed at 970 °C for 40 h and at 300 °C for 40 h in O_2 atmosphere after sintering.

TABLE II. Compositions, lattice parameters, and magnetic-superconducting transition temperatures (T_c) of the samples in the $La_{1+x}Ba_{2-x}Cu_3O_y$ series. (Numbers in parentheses indicate standard deviations.)

Sample No	Composition x	Composition y	Lattice parameters a (Å)	b (Å)	$c/3$ (Å)	c (Å)	V (Å^3)	Magnetic T_c (K)
1	0.00	6.95	3.884(1)	3.939(1)	3.939	11.820(2)	180.81	93
2	0.05	6.98	3.884(1)	3.936(1)	3.936	11.809(2)	180.56	91
3	0.10	6.92	3.889(1)	3.934(1)	3.934	11.805(2)	180.61	86
4	0.20	6.92	3.888(1)	3.934(1)	3.934	11.801(2)	180.50	79
5	0.30	7.04	3.912(1)		3.912	11.736(1)	179.64	70
6	0.00	7.15	3.885(2)	3.934(2)	3.933	11.800(4)	180.35	90
7	0.05	7.13	3.885(2)	3.933(2)	3.932	11.797(4)	180.23	88
8	0.10	7.14	3.898(2)	3.918(2)	3.916	11.747(6)	179.40	79
9	0.20	7.10	3.914(1)		3.915	11.744(1)	179.93	60
10	0.30	7.20	3.912(1)		3.912	11.735(1)	179.58	50
11	0.40	7.15	3.911(1)		3.908	11.733(1)	179.49	50
12	0.50	7.11	3.904(1)		3.905	11.714(5)	178.55	
13	0.10	6.94	3.885(1)	3.931(1)	3.931	11.795(2)	180.13	84
14	0.10	7.04	3.889(1)	3.930(1)	3.930	11.790(4)	180.20	74

Table II and Fig. 1 are the average of two or three determinations.

To confirm the accuracy of the oxygen measurement, the oxygen content of a good quality $YBa_2Cu_3O_y$ sample was measured. This sample showed a sharp superconducting transition and almost 60% Meissner flux exclusion by magnetic-susceptibility measurements. The oxygen content was found to be 6.95, which was in good agreement with the value determined by an iodometric titration technique (6.92).[20]

Polished surfaces of the ceramics were observed using a polarized optical microscope. HRTEM experiments were made using a H-9000 ultrahigh resolution-type high-resolution electron microscope operated at 300 kV.

Electrical resistivity was measured by a conventional four-probe technique. The dc magnetic susceptibility was measured by a superconducting quantum interference device (SQUID) magnetometer (SHE model 905). The measurement was performed by decreasing the temperature from above the superconducting transition point under a fixed field of 10 Oe.

The procedure for thermal analysis (TG and DSC) was reported in detail in a previous paper.[21] Thermal analyses were performed on powder samples. The TG measurements were carried out using a MAC Science model TG-DTA 2000. The measurements were made between 200 and 950 °C at a heating and cooling rate of 10 °C/min and at an O_2 or N_2 gas flow rate of 100 cm^3/min. DSC measurements were carried out using a MAC Science model DSC 3100. The measurements were made between 200 and 600 °C at a heating and cooling rate of 10 °C/min and at an O_2 gas flow rate of 50 cm^3/min.

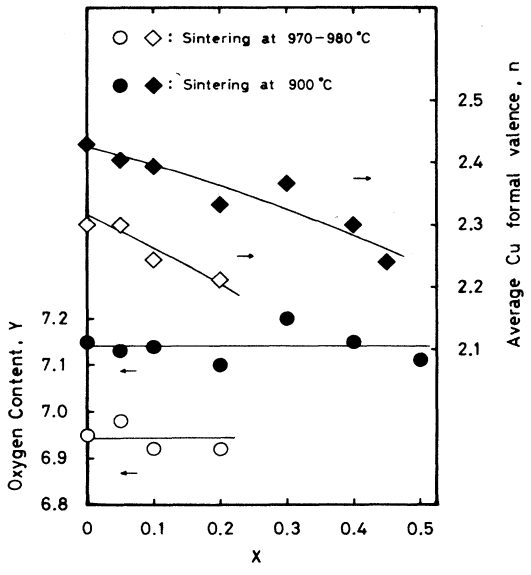

FIG. 1. Oxygen content (y) and average formal copper valence (n) for $La_{1+x}Ba_{2-x}Cu_3O_y$ series.

III. RESULTS

A. Oxygen content and lattice parameters

The x-ray-diffraction patterns indicate that all of the samples shown in Table I are single phase with the tri-perovskite structure.[4] The oxygen contents and crystallographic unit-cell parameters are presented in Table II.

1. Samples 1–5 sintered at 970–980 °C in N_2 gas

For $0 \leq x \leq 0.2$, orthorhombic $La_{1+x}Ba_{2-x}Cu_3O_y$ could be prepared by sintering at 970–980 °C in N_2 gas and postannealing in dry O_2 gas. For $x \geq 0.3$, the obtained ceramics were multiphase; they all contained a second phase with the La_2CuO_4 structure.[22] Sample 5 ($x=0.3$) was prepared by two-step annealing at 970 °C for 40 h and at 300 °C for 40 h in O_2 gas atmosphere after a sintering at 970 °C in N_2 gas. This sample was single phase with tetragonal unit cell.

As La^{3+} is substituted for Ba^{2+} in $LaBa_2Cu_3O_7$,

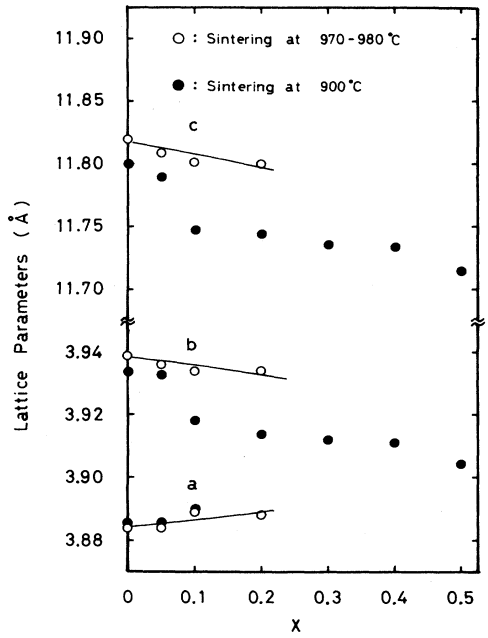

FIG. 2. Lattice parameters for $La_{1+x}Ba_{2-x}Cu_3O_y$ series, determined by x-ray-powder diffraction.

charge compensation may occur either by a reduction of the formal copper valence, by an increase in the oxygen content, or both. The oxygen contents (y) of La_{1+x}-$Ba_{2-x}Cu_3O_y$ samples and their average formal copper valences [$n=(2y-7-x)/3$] are plotted in Fig. 1. For the sample 1-4 sintered at 970-980 °C in N_2 gas, the oxygen contents varied little, ranging between 6.92 and 6.98. Therefore, it follows that the formal copper valence (n) was reduced from 2.30 ($x=0.0$) to 2.21 ($x=0.2$) with increasing excess La content by the charge compensation effect.

The lattice parameters for $La_{1+x}Ba_{2-x}Cu_3O_y$ samples are plotted in Fig. 2. Orthorhombic $La_{1+x}Ba_{2-x}Cu_3O_y$ has a large a-b splitting for small x; with increasing x, the a axis lengthens and the b axis shortens, moving toward tetragonal symmetry. This tendency probably results from depletion of oxygen from the one-dimensional chains parallel to the b axis and population of normally vacant oxygen sites between coppers parallel to a axis. In these orthorhombic samples, the relation $a<b\leq c/3$ holds as in the other orthorhombic $LBa_2Cu_3O_y$ (L is Y or a rare-earth element) materials.[23] The meaning of this rule from the crystallographic point of view has been investigated.[24] Sample 5 with $x=0.3$ was found to be not orthorhombic but tetragonal by x-ray-powder diffraction. The problem of the symmetry of this sample will be discussed later.

2. *Samples 6–12 sintered at 900 °C in N_2 gas*

Single-phase $La_{1+x}Ba_{2-x}Cu_3O_y$ ($0\leq x\leq 0.5$) samples can be prepared using this sintering condition. Their oxygen contents exceeds 7.0, and being fixed at a value near 7.15, as shown in Table II and Fig. 1. The formal copper valence (n) was reduced from 2.43 ($x=0$) to 2.24 ($x=0.5$) with increasing La content. The oxygen contents ($7.10\leq y\leq 7.20$) were considerably larger than those of samples sintered at 970-980 °C. Therefore, the average formal copper valences are higher than those of the samples sintered at 970-980 °C.

The lattice parameters of the samples are also plotted in Fig. 2. For $0\leq x\leq 0.1$, the samples were orthorhombic but their a-b splittings were small. For $0.2\leq x\leq 0.5$, only tetragonal samples could be prepared under these conditions. It is interesting that the $c/3$ is very close to a in all the tetragonal samples. For $x=0.2$, both orthorhombic (sample 4) and tetragonal (sample 9) phases could be prepared. The x-ray-diffraction patterns of these samples are shown in Fig. 3, together with that of orthorhombic sample 1, $La_{1.0}Ba_{2.0}Cu_{3.0}O_{6.95}$. The characteristic peaks between 45° and 48° are shown magnified. The $K\alpha_2$ peaks have been eliminated using a modified Rachinger method.[25,26] The unit-cell volume ($V=a\times b\times c$) decreases with increasing x both in samples sintered at 970-980 °C and in those sintered at 900 °C. The unit-cell volume of the sample sintered at 970-980 °C is lower than that of the sample sintered at 900 °C and the oxygen content of the sample sintered at the higher temperature is lower than that of the sample sintered at the lower temperature. For example, the unit-cell volume of orthorhombic sample 4, $La_{1.2}Ba_{1.8}Cu_3O_{6.92}$, is 180.50 Å^3 and that of tetragonal sample 9, $La_{1.2}Ba_{1.8}Cu_3O_{7.10}$, is 179.93 Å^3.

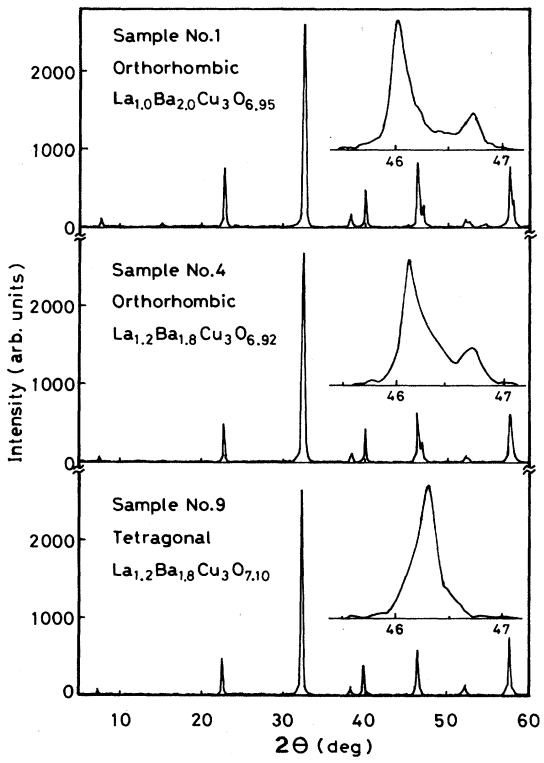

FIG. 3. X-ray-powder-diffraction patterns for some samples in $La_{1+x}Ba_{2-x}Cu_3O_y$ series.

B. Observation of the structure by optical microscopy and high-resolution transmission electron microscopy

Polished surfaces of samples were observed in a cross polarized light microscope; typical examples are shown in Figs. 4(a) and 4(b). These photographs show the surface of the orthorhombic sample 2 with the composition $La_{1.05}Ba_{1.95}Cu_3O_{6.98}$. Grain boundaries and domain boundaries are well discriminated by color differences. Many grains are seen in Fig. 4(a). We believe that the aspect ratio (length/width) of the grains is smaller than that of the rectangular grains in $YBa_2Cu_3O_y$ ceramics.[27,28] Many microdomains in the grains are seen in Fig. 4(b). Similar domain structures have been observed in orthorhombic $YBa_2Cu_3O_y$ ceramics.[27,28] The twin planes are probably (110) planes by analogy with $YBa_2Cu_3O_y$. In the tetragonal samples, twin boundaries are not observed in the grains.

Recently, it was pointed out that x-ray-powder-diffraction analysis is not adequate to discriminate between the orthorhombic and the tetragonal phases for the so-called 1:2:3 compound. For $YBa_2Cu_{1.96}Fe_{0.04}O_y$, the lattice parameters, *a* and *b*, determined by x-ray-powder diffraction appear closer because of interference of scattered waves from adjacent microdomains, even though the real lattice parameters in each microdomain do not change.[29,30]

We intensively studied tetragonal sample 9 with the composition of $La_{1.20}Ba_{1.80}Cu_3O_{7.10}$ by HRTEM, with an accelerating voltage of 300 kV. Figure 5 shows a high-resolution lattice image taken with the incident beam parallel to the *c* axis. This photograph shows that this sample is tetragonal; no twin boundary is observed. Electron-diffraction analysis also suggests that sample 9 is not orthorhombic but tetragonal. The electron-diffraction pattern of orthorhombic sample 4 taken with the incident beam nearly parallel to the *c* axis is shown in Fig. 6. The figure shows spot splitting due to twinning. This type of twinning, with the twin boundary nearly parallel to the (110) planes, is frequently observed in orthorhombic $YBa_2Cu_3O_y$.[31,32]

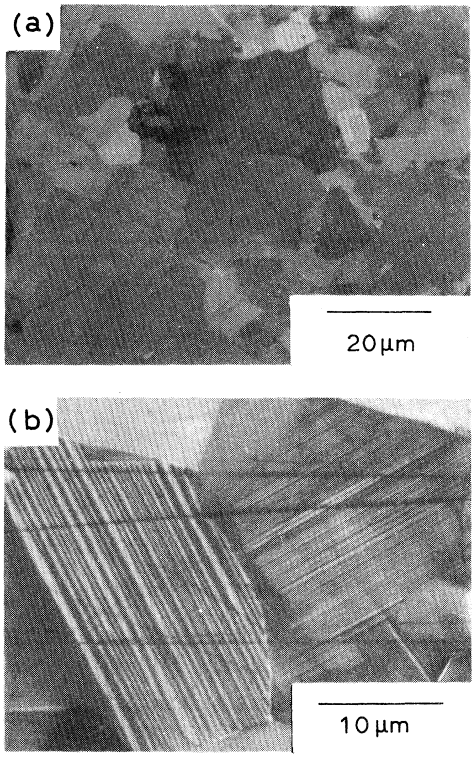

FIG. 4. Typical optical micrographs (polarized light) of polished surface of orthorhombic sample 2, $La_{1.05}Ba_{1.95}Cu_3O_{6.98}$.

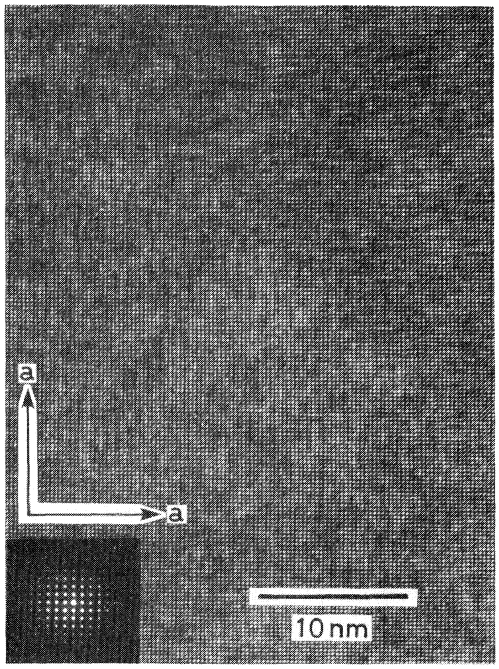

FIG. 5. Lattice image of tetragonal $La_{1.2}Ba_{1.8}Cu_3O_{7.1}$ (sample 9), taken with the incident beam parallel to *c* axis.

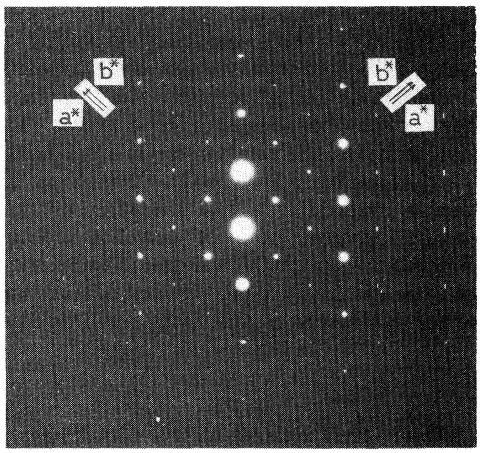

FIG. 6. Electron-diffraction patterns of orthorhombic $La_{1.2}Ba_{1.8}Cu_3O_{6.92}$ (sample 4) with the electron beam parallel to *c* axis.

In sample 9, another type of twinning was observed; a lattice image is shown in Fig. 7. There are three sets of microdomains (*A*, *B*, and *C*) with their *c* axis perpendicular to one another. Similar twinning has been observed in $Nd_{1.5}Ba_{1.5}Cu_3O_y$ (Ref. 33) and $La_{1.5}Ba_{1.5}Cu_3O_y$.[34] This type of twinning is considered to result from the closeness of $a(=3.914\ \text{Å})$ to $c/3(=3.915\ \text{Å})$ and the disorder of La and Ba atoms in the triperovskite structure.[34]

In order to understand the structure of the tetragonal sample, we studied its high-resolution structure image, taken with the incident beam parallel to the *a* axis; it is shown in Fig. 8. A projected ideal structure model is inserted in this figure. La and Ba atoms appear as dark spots, Cu atoms as weak dark spots, and oxygen atoms correspond to bright regions located between the dark spots. Brighter regions indicated by O_X and O_Y are considered to be the positions of oxygen vacancies by analogy with the high-resolution lattice images of $YBa_2Cu_3O_y$.[35] The structure observed in this figure is in good agreement with that of $YBa_2Cu_3O_y$.[35,36]

Sample 9 ($y=7.10$) and 4 ($y=6.92$) were sintered at different temperatures; this explains the residual randomness of La and Ba atoms in sample 9. Therefore, we consider that the larger oxygen content of sample 9 rather than 7.0 is caused by the disorder between La and Ba atoms in the structure. This type of disorder cannot be directly detected by HRTEM observation because La and Ba atoms are difficult to distinguish in HRTEM image. Song *et al.*[6] pointed out from their neutron-diffraction study that the broadening in the diffraction peaks as T_c is decreased is indicative of greater disorder in the La and Ba sites and/or the oxygen configuration. A neutron-powder-diffraction study of the sample sintered at 900 °C in N_2 gas is scheduled for the near future.

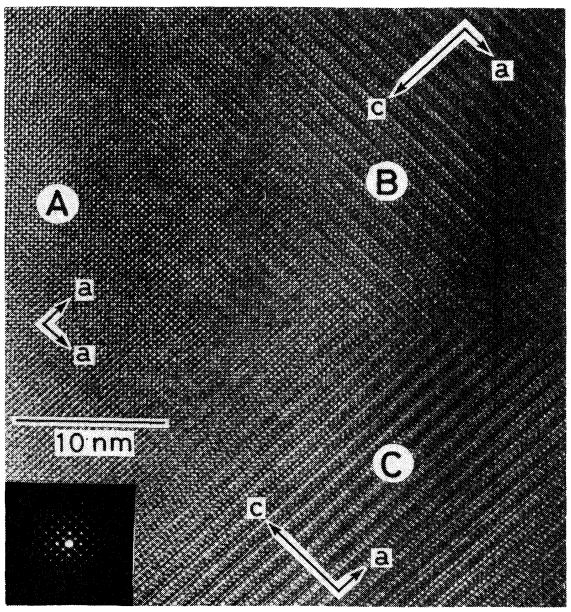

FIG. 7. High-resolution lattice image of tetragonal $La_{1.2}Ba_{1.8}Cu_3O_{7.1}$, showing the three set of microdomains (*A*, *B*, and *C*) with *c* axis perpendicular to one another.

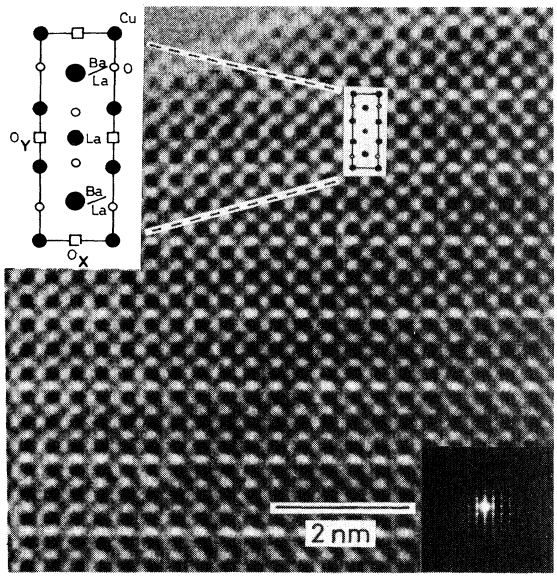

FIG. 8. Structure image of tetragonal $La_{1.2}Ba_{1.8}Cu_3O_{7.1}$, taken with the incident beam parallel to *a* axis. A projected structure model is inserted. Brighter regions indicated by O_X and O_Y are the positions of oxygen vacancies.

C. Oxygen content at elevated temperature

We performed TG measurements in order to study the oxygen contents of the samples at elevated temperature. Figure 9 shows typical TG curves for samples in the $La_{1+x}Ba_{2-x}Cu_3O_y$ series. The thermal treatment was re-

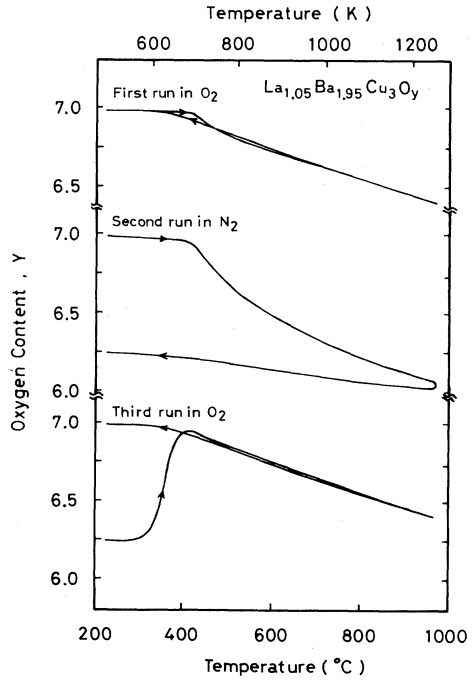

FIG. 9. TG curves of $La_{1.05}Ba_{1.95}Cu_3O_y$ sintered at 970 °C in N_2 gas atmosphere (sample 2) on heating and cooling in O_2 or N_2 gas flow.

peated in O_2, N_2, and O_2 gas flow successively. On the first heating in O_2 gas, $La_{1.05}Ba_{1.95}Cu_3O_{6.95}$ began losing oxygen at 400 °C and was reduced to $y \approx 6.40$ at 950 °C. On the first cooling, it continuously absorbs oxygen down to 300 °C and nearly returns to the original composition, $La_{1.05}Ba_{1.95}Cu_3O_{6.95}$. Hysteresis of TG curves at around 400 °C is seen from this figure. This is due to the difference in oxygen desorption and absorption behavior on heating and cooling. On the second run, in N_2 gas, the compound was reduced to around $La_{1.05}Ba_{1.95}Cu_3O_{6.00}$ at about 950 °C. It did not return to the original composition with $y \approx 7.0$ upon cooling to 200 °C. On the third heating in O_2 gas flow, the reduced material, with $y \approx 6.25$, absorbed a large amount of oxygen in the temperature range between 300 and 400 °C and then again desorbed the oxygen at higher temperature during the first heating. On cooling for the third time, the compound absorbs oxygen again and nearly returns to the original composition, $La_{1.05}Ba_{1.95}Cu_3O_{6.95}$. This TG study shows that $La_{1.05}Ba_{1.95}Cu_3O_y$ desorbs and absorbs oxygen reversibly. The oxygen content at elevated temperature in N_2 gas is considerably lower than that in O_2 gas. For example, at 900 °C, y is about 6.05 in N_2 gas and is 6.40 in O_2 gas.

Figure 10 shows the TG curves of the samples in the $La_{1+x}Ba_{2-x}Cu_3O_y$ series sintered at 970–980 °C upon heating in N_2. This figure shows that the oxygen contents at 900 °C are 6.05, 6.12, 6.20, and 6.30 for the samples with $x=0.0$, 0.1, 0.2, and 0.3, respectively. We see from this result that the samples with higher La content also had higher oxygen contents at elevated temperature. This is considered to be due to presence of La^{3+} ions in the Ba^{2+} sites, presence of excess oxygens brought about by La and Ba disorder, or both. We think that the main cause is the excess positive charge of La^{3+} in the Ba^{2+} site, but we cannot exclude from consideration the effect

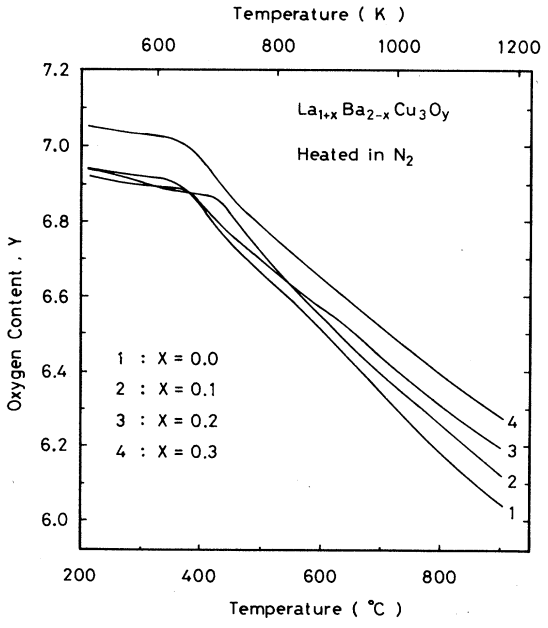

FIG. 10. TG curves of samples in the $La_{1+x}Ba_{2-x}Cu_3O_y$ system sintered at 970–980 °C on heating in flowing N_2 gas.

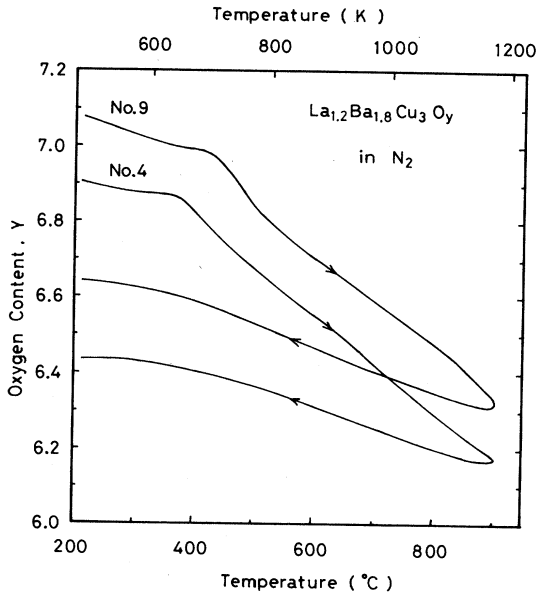

FIG. 11. TG curves of $La_{1.2}Ba_{1.8}Cu_3O_y$ sample sintered under the different conditions on heating in flowing N_2 gas.

of the presence of excess oxygens when attempting to explain results of the DSC study to be discussed in a later section.

Figure 11 shows the TG curves for $La_{1.2}Ba_{1.8}Cu_3O_y$ sintered at 900 °C (sample 9) on heating in N_2, together with the results for orthorhombic sample 4. The oxygen content of sample 9 at 900 °C is 6.35, which is significantly larger than that of sample 4 ($y=6.20$). It is clear that tetragonal sample 9 has oxygen ions which are difficult to remove from the sample.

D. Superconducting properties

1. Samples 1–5 sintered at 970–980 °C in N_2 gas

The temperature dependence of the resistivity is shown in Fig. 12(a). These samples showed metallic temperature dependence of resistivity and sharp superconducting transitions. However, in the case of the samples 4 ($x=0.2$) and 5 ($x=0.3$), which had a large La content, the resistivity showed pronounced tailing below the onset of the superconducting transition. This must be due to degradation of grain boundaries in the ceramics,[12] because these samples show a sharp superconducting transition from magnetic-susceptibility measurement, as shown in Fig. 13(a). The superconducting transition temperature (T_c^{mid}) decreases from 92.5 K ($x=0$) to 70 K ($x=0.3$) with increasing x. These transition temperatures are considerably higher than the previously reported T_c's for samples in the $La_{1+x}Ba_{2-x}Cu_3O_y$ series.[10,13–16]

The temperature dependences of dc magnetic susceptibilities are shown in Fig. 13(a). All the samples 1–5 show bulk superconductivity and their Meissner signals at 10 K are greater than 25% of ideal. The superconducting transition temperatures are 93, 91, 86, 79, and 70 K for

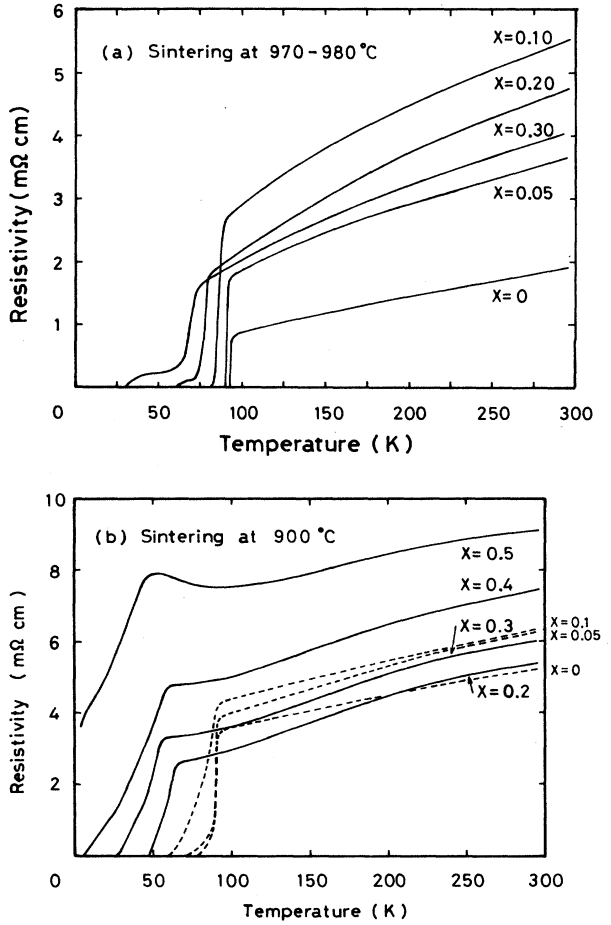

FIG. 12. Temperature dependence of the resistivity for $La_{1+x}Ba_{2-x}Cu_3O_y$ series, (a) samples sintered at 970–980 °C in N_2 gas, (b) samples sintered at 900 °C in N_2 gas.

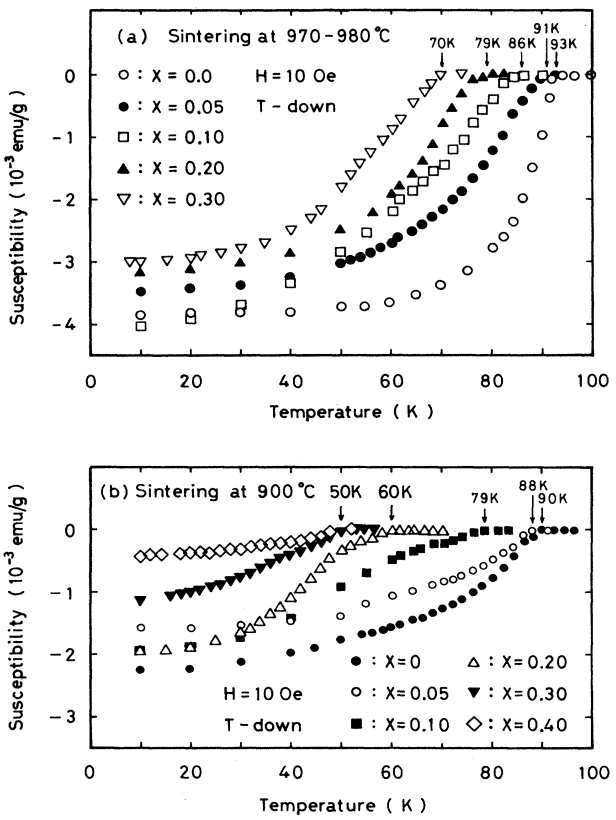

FIG. 13. Temperature dependence of the magnetic susceptibility for $La_{1+x}Ba_{2-x}Cu_3O_y$ series, (a) samples sintered at 970–980 °C in N_2 gas, (b) samples sintered at 900 °C in N_2 gas.

$x=0.0$, 0.05, 0.1, 0.2, and 0.3, respectively. These magnetic T_c's are given in Table II and plotted in Fig. 14(a) against excess La content, x, together with their resistive transition temperatures. These magnetic T_c's are in good agreement with the electrical superconducting transition temperatures. We see that $La_{1+x}Ba_{2-x}Cu_3O_y$ sintered at 970–980 °C shows bulk superconductivity and that the transition temperature is monotonically lowered by substitution of La for Ba.

2. *Samples 6–12 sintered at 900 °C in N_2 gas*

The temperature dependences of resistivities are shown in Fig. 12(b). The orthorhombic samples 6–8 showed metallic temperature dependence of resistivity and a sharp superconducting transition as did the samples sintered at 970–980 °C. The transition temperatures of samples 6–8 were in good agreement with T_c's of samples 1–3 sintered at 970–980 °C. The tetragonal samples 9–12 showed metallic behavior near room temperature but were semiconducting at lower temperatures (below 150 K). Semiconducting behavior was characteristic of samples with higher La contents. They also showed a superconducting transition. The onset temperature of the superconducting transition remained around 50 K for x between 0.2 and 0.5 but the zero-resistance temperature decreased from 47 K ($x=0.2$) to lower than 4 K ($x=0.5$). These superconducting transition temperatures for the tetragonal phase are comparable to reported values.[10,13–16] Resistive T_c's are summarized in Fig. 14(b), together with magnetic T_c's.

The temperature dependence of magnetic susceptibility is shown in Fig. 13(b). The orthorhombic samples 6–8 showed bulk superconductivity at a temperature near the magnetic T_c of the sample sintered at 970–980 °C. However, their superconducting transitions were broader and the volume fraction of superconducting phase, estimated from the values of their Meissner flux exclusions were smaller. The tetragonal sample with $x=0.2$ showed bulk superconductivity with an onset temperature of 60 K. The other tetragonal samples showed superconducting transitions around 50 K but their Meissner signals at 10 K decreased from 1.93×10^{-3} ($x=0.2$) to 3×10^{-5} emu/g ($x=0.5$). The magnetic T_c's found are summarized in Table II and plotted in Fig. 14(b). These magnetic T_c's are in agreement with the onset temperatures of the resistive superconducting transition. We see that the superconducting transition temperatures of samples 9 to 12 were not changed but the volume fraction of supercon-

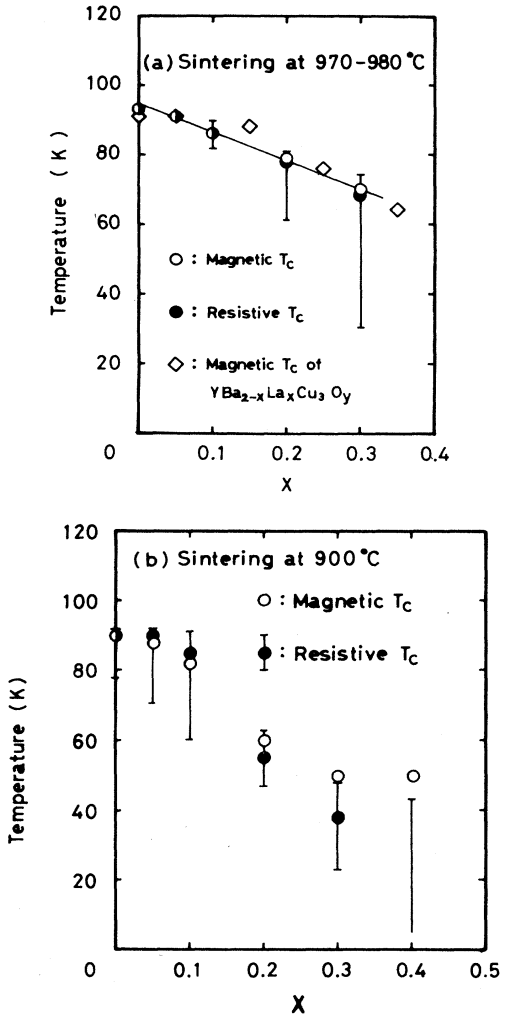

FIG. 14. Resistive and magnetic-superconducting transition temperatures of $La_{1+x}Ba_{2-x}Cu_3O_y$ series, (a) samples sintered at 970–980 °C in N_2 gas, magnetic T_c of $YBa_{2-x}La_xCu_3O_y$ system, determined by Cava *et al.* (Ref. 18) are plotted as well. (b) Samples sintered at 900 °C in N_2 gas.

ducting phase with $T_c \approx 50$ K decreased with increasing La content.

E. Orthorhombic-tetragonal structural phase transition

DSC was performed on samples 1–5. Figure 15 shows typical DSC curves for $La_{1+x}Ba_{2-x}Cu_3O_y$ samples tested in O_2. Heating and cooling between 200 and 600 °C were repeated twice. The endothermic peaks at about 400 °C on heating are due to sudden desorption of O_2 gas from the sample. This sudden absorption of heat was observed by differential thermal analysis (DTA)-TG analysis. Results are shown in Fig. 9. The step at about 476 °C on cooling corresponds to the orthorhombic-tetragonal (O-T) structural phase transition.[21] The endotherm corresponding to desorption of O_2 from the sample is much larger than the discontinuous change in the specific heat at the

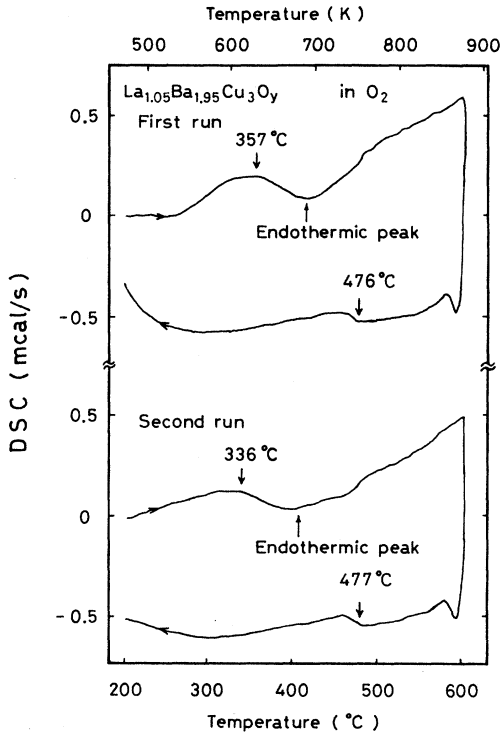

FIG. 15. DSC curve of $La_{1.05}Ba_{1.95}Cu_3O_y$ sintered at 970 °C (sample 2).

second order O-T structural phase transition. Therefore, the step which corresponds to the O-T phase transition was not observed in the DSC curves on heating. On cooling, the exotherm corresponding to absorption of O_2 gas into the sample was not clearly observed in the DSC curves, because the rate of the absorption of O_2 gas into the ceramics did not change suddenly over this temperature range 600 to 300 °C. Hysteresis between desorption and absorption of O_2 at around 400 °C was observed in the TG curve shown in Fig. 9. For this reason, a small anomaly in the heat capacity was clearly observed in the DSC curve on cooling. The sample underwent an O-T phase transition at 476 °C during the first cooling and at 477 °C during the second cooling. This result shows that O-T phase transition in $La_{1+x}Ba_{2-x}Cu_3O_y$ is reversible even at heating and cooling rates as high as 10 °C/min in O_2. However, for some samples, we observed two steps in the DSC curve upon cooling. For example, in sample 2, an upper anomaly occurred at 477 °C and a lower one at 453 °C. This is thought to be due to the difference in O-T transition temperatures of different particles. Thus, the O-T structural phase transition may not always occur at a definite temperature on cooling. The transition from tetragonal to orthorhombic phase is considered to be influenced by the microstructure of the ceramic material.

Similar steps seen on cooling samples in the $La_{1+x}Ba_{2-x}Cu_3O_y$ series are summarized in Fig. 16. The magnitudes of the anomalies in the DSC curves are lowered with increasing excess La content, x. We believe that this is due to the inhomogeneity of the samples with higher La contents, because the orthorhombic $LaBa_2Cu_3O_y$ (sample

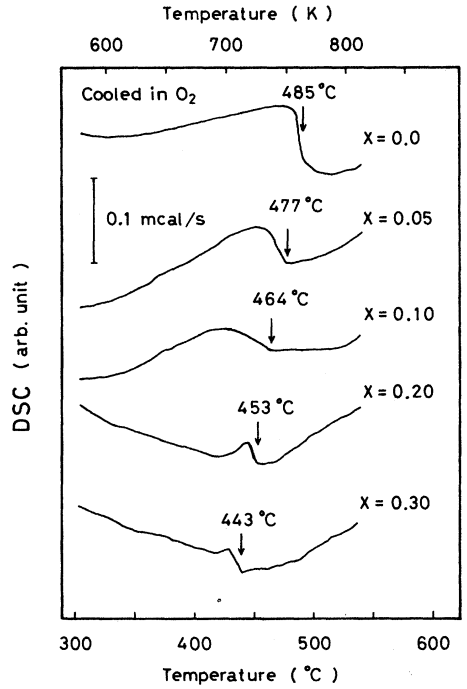

FIG. 16. DSC curves on cooling for $La_{1+x}Ba_{2-x}Cu_3O_y$ series samples sintered at 970–980 °C.

6), which showed a broad superconducting transition from magnetic-susceptibility measurements, showed a broad O-T phase transition from DSC measurements. Sample 5 showed a step in the DSC curve similar to that of orthorhombic samples although it is tetragonal by x-ray-powder diffraction. We believe that if this material were analyzed by neutron-powder diffraction, the occupation factors of oxygen in $(\frac{1}{2},0,0)$ and $(0,\frac{1}{2},0)$ sites would be different. Because the x-ray and electron scattering factors of La and Ba atoms are much larger than those of oxygen, neutron-diffraction analysis should be used for the determination of crystal symmetry in these oxygen-containing materials.[15]

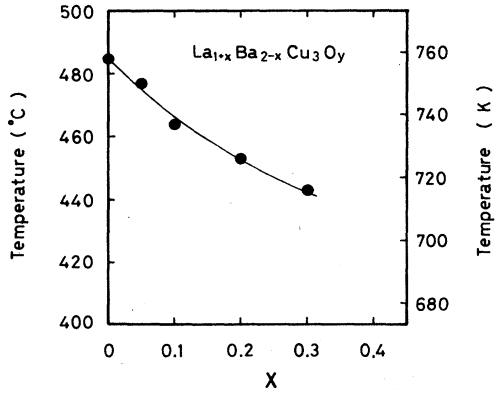

FIG. 17. Orthorhombic to tetragonal structural phase transition temperature for $La_{1+x}Ba_{2-x}Cu_3O_y$ series samples, determined by DSC measurement.

The O-T structural transition temperatures determined are plotted against excess La context, x, in Fig. 17. It is clear that the O-T phase transition temperature decreased almost linearly from 485 °C ($x=0.0$) to 443 °C ($x=0.3$) with increasing x. The smooth curve in Fig. 17 is the phase boundary between orthorhombic and tetragonal phases in the $La_{1+x}Ba_{2-x}Cu_3O_y$ system at an oxygen partial pressure of 1 atm.

IV. DISCUSSION

We will discuss the following three points. The first is the effect of La substitution for Ba in $LaBa_2Cu_3O_y$ on the superconducting properties. The second is the relation between the oxygen content of the samples and their crystallographic and superconducting properties. The last point is why the superconducting properties of the samples, which were sintered at 970–980 °C in N_2 gas and postannealed in dry O_2 gas atmosphere, were so much better than those of the samples sintered in air or O_2.

A. Effect of La^{3+} substitution for Ba^{2+} in orthorhombic $LaBa_2Cu_3O_y$ ($y \approx 7.0$) on the superconducting properties

We will discuss the effect of La^{3+} substitution for Ba^{2+} in orthorhombic $LaBa_2Cu_3O_y$ ($y \approx 7.0$) on the superconducting properties, on the basis of the results of orthorhombic samples 1–4. The bulk T_c of orthorhombic $La_{1+x}Ba_{2-x}Cu_3O_y$ decreases monotonically from 93 to 80 K as the excess lanthanum content, x, increases to 0.2. However, we know that the substitution of La^{3+} for Ba^{2+} in $LaBa_2Cu_3O_y$ does not substantially affect the oxygen content or crystal structure. Therefore, we feel that the lowering of T_c in these samples is due to the decrease in the carrier density since the T_c of an oxide superconductor has been correlate with the carrier(hole) density.[37]

Similar results were reported in the $YBa_{2-x}La_xCu_3O_y$ ($y \approx 7.0$) system.[18] The T_c's of orthorhomic $YBa_{2-x}La_xCu_3O_y$ ($y \approx 7.0$), determined magnetically by Cava *et al.*,[18] are plotted in Fig. 14(a) together with the data for orthorhombic $La_{1+x}Ba_{2-x}Cu_3O_y$. The figure shows that the T_c of orthorhombic $La_{1+x}Ba_{2-x}Cu_3O_y$ is in good agreement with that of $YBa_{2-x}La_xCu_3O_y$ for equal excess lanthanum contents. Taking account of their equal oxygen contents and their equal resultant average formal copper valences, we think that this result supports the idea that the T_c of the 1:2:3 compound depends on carrier density.

B. Relation between the oxygen content and the crystallographic and superconducting properties in $La_{1+x}Ba_{2-x}Cu_3O_y$ system

Our results on the relation between the oxygen content of the samples and their crystallographic and superconducting properties can be summarized as follows.

(1) The samples with lower oxygen contents ($y \leq 7.0$) were prepared by sintering at 970–980 °C in N_2 gas and the ones with higher oxygen content ($y > 7.0$) were prepared by sintering at 900 °C in the same atmosphere.

(2) Regardless of the oxygen content of the samples, they all had a triperovskite structure.

(3) The samples with higher oxygen content tended to be tetragonal and had a shorter c axis, whether they are orthorhombic or tetragonal.

(4) Samples with $0 \leq x \leq 0.1$ were all orthorhombic and had almost equal T_c's, but samples with higher oxygen content showed broader superconducting transitions and had smaller Meissner signals.

(5) For the tetragonal samples with higher oxygen content, the T_c's were low and the Meissner signals were small.

(6) We believe that the excess oxygen occupies the vacancies in the triperovskite structure because of disorder in the (Ba/La)-La-(Ba/La) sequence along the c axis.

We suspect that the excess oxygen occupying O_X sites reduces the difference between the occupation factors of oxygen at $(\frac{1}{2},0,0)$ and $(0,\frac{1}{2},0)$. This effect reduces the difference of a and b cell dimensions of the unit cell.[38,39] Therefore, samples with $y > 7.0$ tend to become tetragonal. The extrapolation the curve of the dependence of c cell dimension on oxygen content in $YBa_2Cu_3O_y$ $(6.0 \leq x \leq 7.0)$[40] suggests that the extra oxygen occupying O_X sites shortens the c cell dimension. At present, we are not able to explain the effect of the disorder of the (Ba/La)-La-(Ba/La) sequence along c axis or the resultant excess oxygen on the crystal symmetry and c cell dimension of the unit cell.

We believe that the superconducting properties are more strongly affected by disorder in the (Ba/La)-La-(Ba/La) sequence and resultant occupation of O_Y sites by excess oxygen. Metallic but nonsuperconducting $La_{2-x}A_{1+x}Cu_2O_y$ (A=Ca,Sr) has an oxygen-deficient double perovskite structure,[41] which resembles the structure of the high-T_c superconducting oxides $(BiO)_2Sr_2CaCu_2O_y$ or $(TlO)_2Ba_2CaCu_2O_y$.[42,43] The carrier (hole) is doped into $La_{2-x}A_{1+x}Cu_2O_y$ (A=Ca,Sr) by increasing y from 6.0 to 6.2. The excess oxygen occupies the vacant sites between pyramids; they are then connected together at the vertices. Tokura[44] suggested that disordering or connection of pyramids may be incompatible with superconductivity.

Recently, Song *et al.*[45] studied the correlation of T_c with the oxygen content in the $LaBa_2Cu_3O_y$ system and demonstrated that the T_c's of the samples with excess oxygen content ($y > 7.0$) were below 44 K. They suggested that this behavior could be explained by disorder of the La and Ba ions,[6] leading to disruption of the Cu-O chains in the outer Cu-O plane. Their interpretation is in good agreement with our present analysis.

C. Preparation condition of a high-quality $La_{1+x}Ba_{2-x}Cu_3O_y$

In a previous paper,[11,12] we described a technique for reproducible preparation of $LaBa_2Cu_3O_y$ with excellent superconducting characteristics. Our preparation method consisted of the following three procedures: (i) preheat treatment of La_2O_3 powder, (ii) sintering in N_2, and (iii) low-temperature annealing in dry O_2. Further, it has been shown in this paper that (iv) sintering at high temperature (970–980 °C) is required for preparation of high-quality samples. In the previous paper,[11,12] we discussed the effects of processes (i) and (iii) only. We did not discuss why the superconducting properties of the samples which were sintered in N_2 were so much better than those of the samples sintered in air or O_2 gas atmosphere. Here, we will discuss processes (ii) and (iv) in detail.

First, we will discuss the effect of the sintering atmosphere on the phases present in the $La_{1+x}Ba_{2-x}Cu_3O_y$ system. It is known that a homogeneous single-phase sample can be prepared in the range from $x=0.1$ to 0.6 at about 950 °C in air or O_2 (Refs. 13 and 14) and that for the starting composition $LaBa_2Cu_3O_y$, the sample always contains a small amount of $BaCuO_2$ as an impurity phase. From the phase rule we saw that the phases present in the sample might be dependent on the sintering atmosphere, and concluded that single-phase $LaBa_2Cu_3O_y$ might be prepared by control of the sintering atmosphere. Homogeneous solid solutions in the $La_{1+x}Ba_{2-x}Cu_3O_y$ series can be prepared in the range from $x=0.0$ to 0.5 at 900 °C in N_2 and in the range from $x=0.0$ to 0.2 at 970 °C in the same atmosphere. In N_2 gas atmosphere, stoichiometric $LaBa_2Cu_3O_y$ without second-phase impurities can be synthesized; the x-ray-diffraction pattern of such a material is shown in Fig. 3. To clarify the phase boundary between the triperovskite phase ($La_{1+x}Ba_{2-x}Cu_3O_y$) and second-phase material at 900 °C in a N_2 gas atmosphere, we fired $La_{1-x}Ba_{2+x}Cu_3O_y$ ($x=0.05$ and 0.10) samples at 900 °C in N_2. The x-ray-diffraction patterns indicated that these samples contained a small amount of $BaCuO_2$ as a second-phase impurity. We see that the phase boundary of the triperovskite phase in the Ba rich region is close to $x=0$ and that the coexisting phase is $BaCuO_2$. Abbattista[46] studied equilibrium relationships in the barium-rich part of the BaO-CuO-O_2 system and showed that $BaCuO_2$ is stable in an inert gas atmosphere (e.g., Ar gas). Thermal analyses (DTA-TG and DSC) in air showed that $BaCuO_2$ and $La_{1.1}Ba_{1.9}Cu_3O_y$ melt at about 1000 °C and 1060 °C, respectively. Thermal analyses in N_2 gas showed that $BaCuO_2$ and $La_{1.0}Ba_{2.0}Cu_3O_y$ melt in a reducing atmosphere at 920 °C and 1000 °C, respectively.

We assume from the phase that N_2 gas does not directly influence the sample during the sintering but that sintering under low oxygen partial pressure is important. To confirm our prediction, we prepared $LaBa_2Cu_3O_y$ by sintering in Ar at 970 °C. We obtained a single-phase sample. This result is in good agreement with our prediction. Therefore, we conclude that one of the requirements for the preparation of stoichiometric $LaBa_2Cu_3O_y$ is sintering at 900–980 °C in a low-oxygen partial pressure atmosphere. This is one of the most important processes for the preparation of high-T_c samples in the $La_{1+x}Ba_{2-x}Cu_3O_y$ system, because the superconducting properties degrade with increasing excess La content, x.[10,13–16]

We prepared samples 13 and 14 with the composition of $La_{1.1}Ba_{1.9}Cu_3O_y$, in order to compare the effect of sintering atmosphere on the superconducting properties. The samples were sintered in Ar gas and air, respectively. The sintering temperature and annealing condition were the same as for sample 3. The compositions and preparation conditions are shown in Table I and the lattice parameters

and magnetic T_c's are summarized in Table II. The oxygen content of sample 13 sintered in Ar gas was 6.94; this is as large as that of sample 3 ($y=6.92$). The oxygen content of sample 14 ($y=7.04$) was substantially larger than that of sample 3. Sample 13 was orthorhombic and had lattice parameters comparable with those of sample 3. Sample 14 was orthorhombic but had a very small a-b splitting and a c value shorter than that of sample 3. The temperature dependences of the magnetic susceptibilities of samples 3, 13, and 14 are shown in Fig. 18. The T_c of sample 14 was considerably lower than those of samples 3 and 13. We see from these results that sintering under low-oxygen partial pressure, for example, in N_2 or Ar, contributes to good superconducting properties in the $La_{1.1}Ba_{1.9}Cu_3O_y$ system.

We will now discuss the effect of sintering at low-oxygen partial pressure from a structural point of view. It is seen from Fig. 9 that $La_{1.05}Ba_{1.95}Cu_3O_{6.92}$ is reduced to $y=6.4$ at 950 °C in O_2 gas atmosphere and reduced to $y\approx 6.0$ at 950 °C in a N_2 gas atmosphere. Now we consider the bond valence sum[47,48] at the La and Ba sites in $LaBa_2Cu_3O_y$. The bond valence sums for Y site and Ba site in $YBa_2Cu_3O_y$ (Ref. 4) are calculated using the method of Brown and Altermatt,[47] because structural data for the reduced $LaBa_2Cu_3O_y$ is not available at present. The calculated values for Y and Ba sites in orthorhombic $YBa_2Cu_3O_{6.69}$ and tetragonal $YBa_2Cu_3O_{6.32}$ are given in Table III. In orthorhombic $YBa_2Cu_3O_{6.69}$, the bond valence sum for the Y site is 2.85 and that for Ba site is 2.08; the difference is thus 0.77. In reduced $YBa_2Cu_3O_{6.32}$, the value for the Y site is 2.91 and that for the Ba site is 1.91; the difference is thus 1.0. The difference between the bond valence sums of Y and Ba sites in the reduced composition is clearly larger than that in the oxidized composition. This result shows why the La and Ba atoms more readily become ordered in the reduced composition. This is considered to be one of the reasons why the ordering of La and Ba along the c axis proceeds more quickly during sintering in a low-oxygen partial pressure atmosphere.

We will then discuss the materials from the kinetic point of view. The reduced materials, for example, $La_{1.05}$-

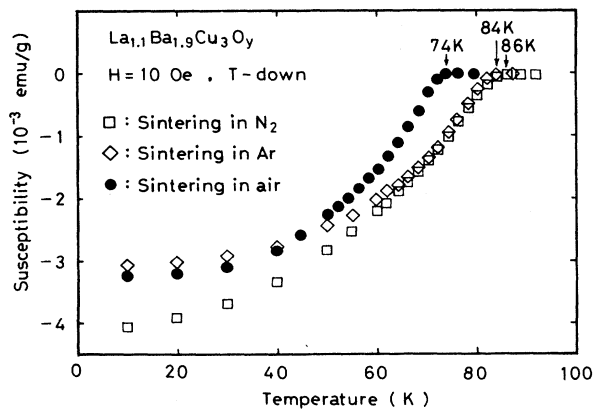

FIG. 18. Temperature dependence of magnetic susceptibility of samples 3, 13, and 14 which were sintered at 970 °C in N_2 gas, Ar gas, and air, respectively.

TABLE III. Bond valence sums (Ref. 47) for Y and Ba sites in orthorhombic $YBa_2Cu_3O_{6.69}$ and tetragonal $YBa_2Cu_3O_{6.32}$ (Ref. 4).

	$YBa_2Cu_3O_{6.69}$	$YBa_2Cu_3O_{6.32}$
Y site	2.85	2.91
Ba site	2.08	1.91
difference	0.77	1.00

$Ba_{1.95}Cu_3O_{6.0}$ fired at 950 °C in N_2 gas atmosphere, has many oxygen vacancies and has a larger unit cell because of its lower oxygen concentration. Therefore, we believe that the diffusion rate of La or Ba in the perovskite structure is larger in the reduced material and that the ordering of La and Ba is thus achieved within a shorter heating period. We think that this is also one of the reasons why sintering in a N_2 gas atmosphere accelerates the ordering of La and Ba in the perovskite structure.

Diffusion usually proceed more rapidly at higher temperatures. Since ordering of La and Ba atoms occurs by diffusion, we conclude that a fourth requisite for preparation of high-quality $La_{1+x}Ba_{2-x}Cu_3O_y$ samples is sintering at high temperature (980–970 °C).

V. CONCLUSION

$La_{1+x}Ba_{2-x}Cu_3O_y$ samples with $0\leq x\leq 0.2$ were prepared by sintering at 970–980 °C in N_2 gas and postannealing at 300 °C in dry O_2. The samples were all orthorhombic.

$La_{1+x}Ba_{2-x}Cu_3O_y$ samples with $0\leq x\leq 0.5$ were prepared by sintering at 900 °C in N_2 gas and postannealing at 300 °C in dry O_2. The samples with $0\leq x\leq 0.1$ were orthorhombic and those with $0.2\leq x\leq 0.5$ were tetragonal.

The oxygen contents of the samples sintered at 970–980 °C were about 6.95 and those of the samples sintered at 900 °C were larger than 7.0, typically about 7.15.

$La_{1+x}Ba_{2-x}Cu_3O_y$ samples sintered at 970–980 °C had better superconducting properties. All samples show a sharp superconducting transition and their Meissner flux exclusion at 10 K was more than 25% of the ideal value.

The superconducting transition temperatures of La_{1+x}-$Ba_{2-x}Cu_3O_y$ samples with $y\approx 6.95$ decreased linearly from 93 K ($x=0.0$) to 70 K ($x=0.3$) with increasing excess La content, x.

The orthorhombic-tetragonal structural phase transition temperature in $La_{1+x}Ba_{2-x}Cu_3O_y$ samples with $y\approx 6.95$ decreased monotonically from 485 °C ($x=0.0$) to 443 °C ($x=0.3$) with excess La content, x.

In order to obtain $La_{1+x}Ba_{2-x}Cu_3O_y$ samples with good superconducting properties, we must prepare samples with the triperovskite structure in which La and Ba have an ordered arrangement along the c axis and the occupation factors of oxygen at $(\frac{1}{2},0,0)$ and $(0,\frac{1}{2},0)$ are close to 0 and 1, respectively.

ACKNOWLEDGMENTS

We thank H. Takagi of University of Tokyo and Dr. H. Yamauchi of International Superconductivity Technology

Center for their helpful discussions and Dr. M. Izumi of Tokyo University of Mercantile Marine for useful discussions about the crystallographic analysis. We thank Dr. W. C. Moffatt of International Superconductivity Technology Center for a critical reading of the manuscript. We also thank T. Maeda of The Furukawa Electric Co. Ltd. and H. Naganuma of Matsushita Technoresearch Inc. for oxygen analyses, and Dr. F. Nagata of Hitachi Instrument Engineering Co. Ltd. for high resolution electron microscopy. We also acknowledge the technical assistance of S. Takebayashi of University of Tokyo.

[1]A. Maeda, T. Yabe, K. Uchinokura, and S. Tanaka, Jpn. J. Appl. Phys. **26**, L1368 (1987).
[2]S. I. Lee, J. P. Golben, S. Y. Lee, X. D. Chen, Y. Song, T. Y. Noh, R. D. McMichael, J. R. Gaines, D. L. Cox, and B. R. Patten, Phys. Rev. B **36**, 2417 (1987).
[3]M. Izumi, A. Maeda, K. Uchinokura, T. Yabe, H. Asano, F. Izumi, T. Wada, T. Hasegawa, and S. Tanaka, Physica C **153-155**, 964 (1988).
[4]F. Izumi, H. Asano, T. Ishigaki, E. Muromachi, Y. Uchida, N. Watanabe, and T. Nishikawa, Jpn. J. Appl. Phys. **26**, L649 (1987).
[5]M. A. Beno, L. Soderholm, D. W. Capone, D. G. Hinks, J. D. Jorgensen, I. K. Shuller, C. V. Segre, K. Zhang, and J. D. Grace, Appl. Phys. Lett. **51**, 57 (1987).
[6]Y. Song, J. P. Golben, S. Chittipeddi, S. I. Lee, R. D. McMichael, X. D. Chen, J. R. Gaines, and D. L. Cox, Phys. Rev. B **37**, 607 (1988).
[7]Y. Matsui, Y. Kitami, M. Yokoyama, N. Iyi, E. Muromachi, and S. Takekawa, J. Electron Microsc. **36**, 246 (1987).
[8]R. Yoshizaki, H. Sawada, T. Iwazumi, Y. Saito, Y. Abe, H. Ikeda, K. Imai, and I. Nakai, Jpn. J. Appl. Phys. **26**, L1703 (1987).
[9]Q. Li, C. Y. Li, K. Wu, and D. Yin, Solid State Commun. **64**, 1133 (1987).
[10]S. A. Sunshine, L. F. Schneemeyer, J. V. Waszczak, D. W. Murphy, S. Miraglia, A. Santoro, and F. Beech, J. Cryst. Growth **85**, 632 (1987).
[11]T. Wada, N. Suzuki, T. Maeda, A. Maeda, S. Uchida, K. Uchinokura, and S. Tanaka, Appl. Phys. Lett. **52**, 1989 (1988).
[12]A. Maeda, T. Noda, H. Matsumoto, T. Wada, M. Izumi, T. Yabe, K. Uchinokura, and S. Tanaka, J. Appl. Phys. **64**, 4095 (1988).
[13]C. Dong, J. K. Liang, G. C. Che, S. S. Xie, Z. X. Zao, Q. S. Yang, Y. M. Ni, and G. R. Liu, Phys. Rev. B **37**, 5182 (1988).
[14]E. Muromachi, Y. Uchida, A. Fujimori, and K. Kato, Jpn. J. Appl. Phys. **26**, L1546 (1987).
[15]C. U. Segre, B. Dabrowski, D. G. Hinks, K. Zhang, J. D. Jorgensen, M. A. Beno, and I. K. Shuller, Nature (London) **329**, 227 (1987).
[16]M. Onoda, K. Fukuda, M. Sera, and M. Sato, Solid State Commun. **64**, 1225 (1987).
[17]R. D. Shanon, Acta Crystallogr. A **32**. 751 (1976).
[18]R. J. Cava, B. Batlogg, R. M. Fleming, S. A. Sunshine, A. Ramirez, E. A. Rietman, S. M. Zahurak, and R. B. van Dover, Phys. Rev. B **37**, 5912 (1988).
[19]M. U. Cohen, Rev. Sci. Instrum. **6**, 68 (1935); **7**, 155 (1936).
[20]K. Kishio, J. Shimoyama, T. Hasegawa, K. Kitazawa, and K. Fueki, Jpn. J. Appl. Phys. **26**, L1228 (1987).
[21]T. Wada, N. Suzuki, T. Maeda, A. Maeda, S. Uchida, K. Uchinokura, and S. Tanaka, Phys. Rev. B **38**, 7080 (1988).
[22]J. M. Longo and P. M. Laccah, J. Solid State Chem. **6**, 526 (1973).
[23]H. Asano, K. Takita, H. Katoh, H. Akinaga, T. Ishigaki, M. Nishino, M. Imai, and K. Masuda, Jpn. J. Appl. Phys. **26**, L1410 (1987).
[24]M. Izumi (unpublished).
[25]J. Ladell, A. Zagofsky, and S. Pearlman, J. Appl. Cryst. **8**, 499 (1975).
[26]G. Platbrood, J. Appl. Cryst. **16**, 24 (1983).
[27]M. Murakami, K. Doi, and S. Matsuda, J. Ceram. Soc. Jpn. **96**, 471 (1988).
[28]H. Ledbetter, J. Met. **41**, 24 (1988).
[29]Z. Hiroi, M. Takano, Y. Takeda, R. Kanno, and Y. Bando, Jpn. J. Appl. Phys. **27**, L580 (1988).
[30]G. Roth, G. Heger, B. Renker, J. Pannetier, V. Caignaert, M. Hervieu, and B. Raveau, Z. Phys. B **71**, 43 (1988).
[31]Y. Syono, M. Kikuchi, K. Oh-ishi, K. Hiraga, H. Arai, Y. Matsui, N. Kobayashi, T. Sasaoka, and Y. Muto, Jpn. J. Appl. Phys. **26**, L498 (1987).
[32]S. Ikeda, T. Hatano, A. Matsushita, T. Matsumoto, and K. Ogawa, Jpn. J. Appl. Phys. **26**, L729 (1987).
[33]Y. Matsui, S. Takekawa, and N. Iyi, Jpn. J. Appl. Phys. **26**, L1693 (1987).
[34]K. Suzuki, M. Ichihara, S. Takeuchi, H. Takeya, and H. Takei, Jpn. J. Appl. Phys. **27**, L814 (1988).
[35]K. Hiraga, D. Shindo, M. Hirabayashi, M. Kikuchi, K. Oh-ishi, and Y. Syono, Jpn. J. Appl. Phys. **26**, L1071 (1987).
[36]K. Hiraga, D. Shindo, M. Hirabayashi, M. Kikuchi, and Y. Syono, J. Electron Microsc. **36**, 261 (1987).
[37]M. W. Shafer, T. Penny, and B. L. Olson, Phys. Rev. B **36**, 4047 (1987).
[38]W. I. F. David, W. T. A. Harrison, R. M. Ibberson, M. T. Weller, J. R. Grasmeder, and P. Lanchester, Nature (London) **328**, 328 (1987).
[39]J. D. Jorgensen, B. W. Veal, W. K. Kwok, G. W. Crabtree, A. Umezawa, L. J. Nowicki, and A. P. Paulikas, Phys. Rev. B **36**, 5731 (1987).
[40]A. Ono and Y. Ishizawa, Jpn. J. Appl. Phys. **26**, L1043 (1987).
[41]N. Nguyen, L. Er-Rakho, C. Michel, J. Choisnet, and B. Raveau, Mater. Res. Bull. **15**, 891 (1980).
[42]M. A. Subramanian, C. C. Torardi, J. C. Calabrese, J. Gopalakrishnan, K. J. Morrissey, T. R. Askew, R. B. Flippen, U. Chowdhry, and A. W. Sleight, Science **239**, 1015 (1988).
[43]M. A. Subramanian, J. C. Calabrese, C. C. Torardi, J. Gopalakrishnan, T. R. Askew, R. B. Flippen, K. J. Morrissey, U. Chowdhry, and A. W. Sleight, Nature (London) **332**, 420 (1988).
[44]Y. Tokura, Parity **3**, No. 5, 60 (1988).
[45]Y. Song, J. P. Golben, X. D. Chen, J. R. Gaines, M. S. Wong, and E. R. Kreidler, Phys. Rev. B **38**, 2858 (1988).
[46]F. Abbattista, M. Vallino, C. Brisi, and M. Lucco-Borlera, Mater. Res. Bull. **23**, 1509 (1988).
[47]I. D. Brown and D. Altermatt, Acta Crystallogr. B **41**, 244 (1985).
[48]I. Nakai, K. Imai, T. Kawashima, and R. Yoshizaki, Jpn. J. Appl. Phys. **26**, L1244 (1987).

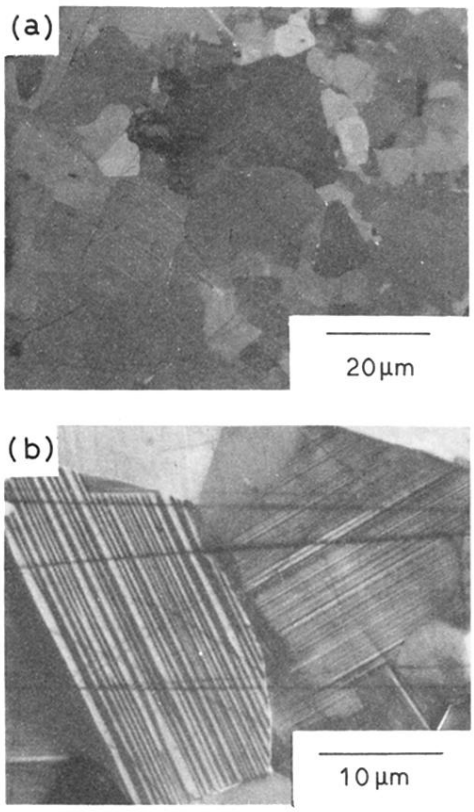

FIG. 4. Typical optical micrographs (polarized light) of polished surface of orthorhombic sample 2, $La_{1.05}Ba_{1.95}Cu_3O_{6.98}$.

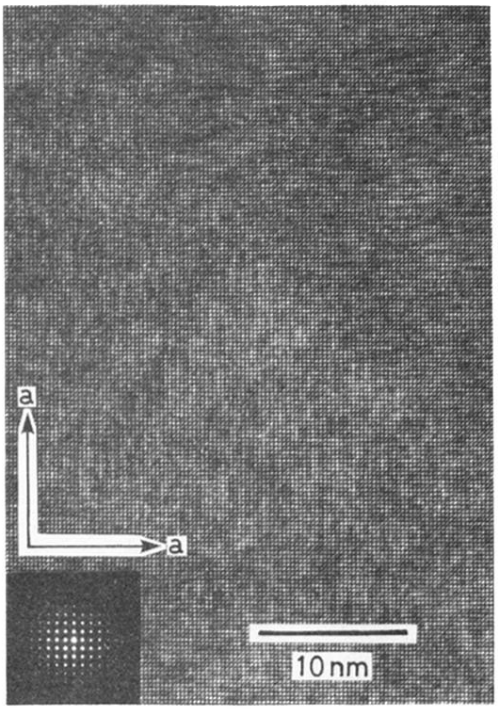

FIG. 5. Lattice image of tetragonal $La_{1.2}Ba_{1.8}Cu_3O_{7.1}$ (sample 9), taken with the incident beam parallel to *c* axis.

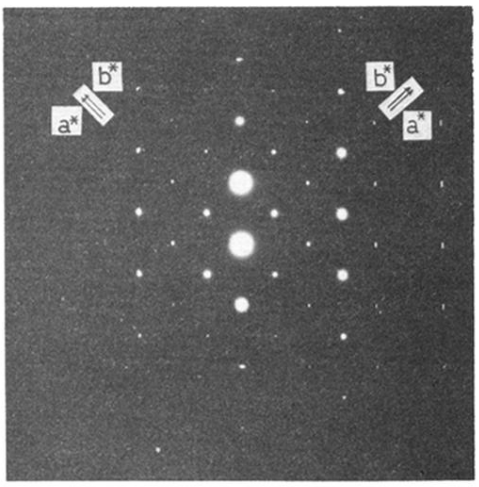

FIG. 6. Electron-diffraction patterns of orthorhombic $La_{1.2}Ba_{1.8}Cu_3O_{6.92}$ (sample 4) with the electron beam parallel to c axis.

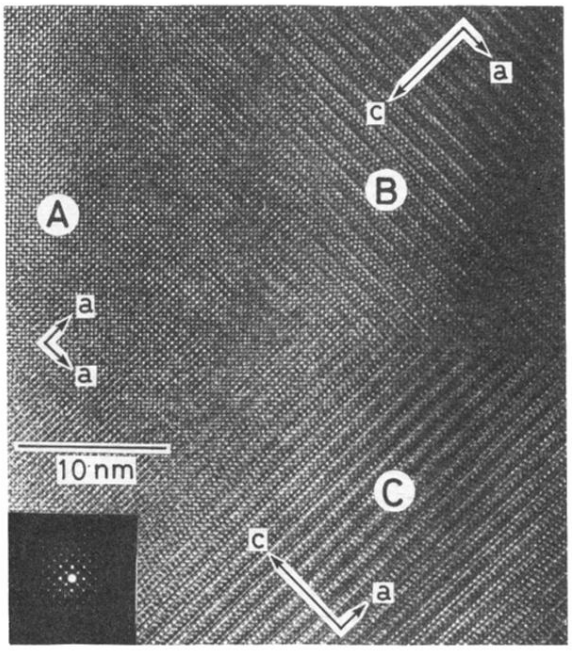

FIG. 7. High-resolution lattice image of tetragonal $La_{1.2}Ba_{1.8}Cu_3O_{7.1}$, showing the three set of microdomains (*A*, *B*, and *C*) with *c* axis perpendicular to one another.

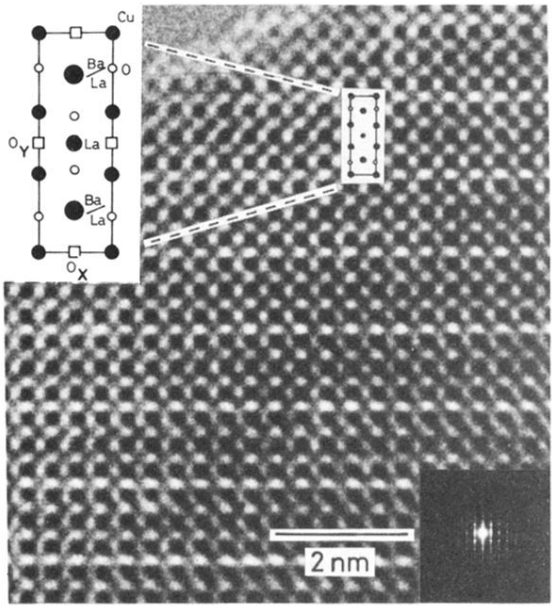

FIG. 8. Structure image of tetragonal $La_{1.2}Ba_{1.8}Cu_3O_{7.1}$, taken with the incident beam parallel to a axis. A projected structure model is inserted. Brighter regions indicated by O_X and O_Y are the positions of oxygen vacancies.